

# SIMULATION OF THE LSD RESPONSE TO THE NEUTRINO BURST FROM SN 1987A

*K. V. Manukovskiy*<sup>a\*</sup>, *A. V. Yudin*<sup>a,b\*\*</sup>, *N. Yu. Agafonova*<sup>c\*\*\*</sup>, *A. S. Malgin*<sup>c</sup>,  
*O. G. Ryazhskaya*<sup>c</sup>

<sup>a</sup> NRC “Kurchatov Institute” — Institute for Theoretical and Experimental Physics, Moscow, 117218 Russia

<sup>b</sup> NRC “Kurchatov Institute”, Moscow, 123182 Russia

<sup>c</sup> Institute for Nuclear Research, Russian Academy of Sciences, Moscow, 117312 Russia

Using the GEANT4 code, we have performed a full-scale simulation of the LSD response to the neutrino burst from SN 1987A. The neutrino flux parameters were chosen according to one of the models: the standard collapse model or the rotational supernova explosion model. We showed that, depending on the chosen parameters, one can either obtain the required number of pulses in the detector or reproduce their energy spectrum, but not both together. The interaction of neutrino radiation both with LSD itself and with the material of the surrounding soil was taken into account in our simulation. We also explored the hypothesis that the entire unique LSD signal at 2:52 UT was produced by neutron fluxes from the surrounding granite. However, this hypothesis was not confirmed by our simulation. The results obtained provide a rich material for possible interpretations.

## 1. INTRODUCTION

Supernova (SN) 1987A exploded on February 23, 1987, triggered a rapid development of the SN explosion theory and experimental neutrino detection methods. This SN was discovered in the optical range [1] and then was observed in all ranges of the electromagnetic spectrum. However, in addition, it was detected by four neutrino detectors: the scintillation, LSD [2] and BUST [3], and Cherenkov, IMB [4] and Kamiokande II (hereafter KII) [5], ones. It should be emphasized that this is the first and so far, unfortunately, the sole case of neutrino detection from supernovae.

The LSD signal from SN 1987A recorded approximately 5 h before the IMB, KII, and BUST detector signals still provokes debates about its origin. In the universally accepted standard collapse model (a spherically symmetric nonrotating star) [6, 7] the neutrino radiation must be a single one, with a duration  $\sim 10$  s, and, therefore, the signal in LSD must be observed simultaneously with the signals in the remaining detectors. In addition, the number of pulses in LSD must be smaller than that in IMB and KII, because the masses of the IMB (5000 t of H<sub>2</sub>O) and KII (2140 t of H<sub>2</sub>O) working material are greater than the LSD mass (90 t of C<sub>n</sub>H<sub>2n</sub>). It is worth noting that all these detectors were designed to detect electron antineutrinos.

However, there are models [8–11] that also admit a double neutrino burst from the SN. As was shown in [12], the signal at 2:52 UT recorded only in LSD and containing five pulses can be explained in terms of the rotating collapsar model [10] as a result of the interaction of high-energy electron neutrinos with the detector structural elements that contained  $\sim 170$  t of iron.

Besides, a similarity of the LSD signal energy characteristics to the spectrum of gamma-ray photons from neutron captures by iron nuclei,  $n + {}^{56}\text{Fe} \rightarrow {}^{57}\text{Fe} + \gamma$  [13], engages our attention. Could the soil surrounding the detector (Mont Blanc granite) irradiated by neutrino fluxes from the SN become a source of neutrons from  $\nu A$  interactions? These neutrons could be captured by the LSD metal structures and produce gamma-ray photons.

---

\* E-mail: manu@itep.ru

\*\* E-mail: yudin@itep.ru

\*\*\* E-mail: agafonova@inr.ru

Given that the range of a gamma-ray photon with a typical energy of 8 MeV in iron is  $\sim 4$  cm, such gamma-ray photons can freely escape from the detector structures and produce a signal in the scintillation counters. This possibility needs to be carefully checked.

A significant uncertainty in the parameters of the neutrinos (especially their energy) emitted during the core collapse of a rapidly rotating SN in the absence of convincing numerical simulations makes an attempt to solve the inverse problem meaningful. That is we can attempt to answer the following question: if all five LSD pulses are attributable to the interaction of neutrino radiation from SN1987A, then what characteristics should it have possessed? This question can be answered only through a direct simulation of the neutrino interaction with the LSD material and surrounding soil.

The goal of our study is to simulate the LSD response to neutrino radiation from SN 1987A within two possible scenarios:

- “standard” collapse with a mean neutrino energy  $\langle E \rangle_{\bar{\nu}_e} \sim 15$  MeV;
- the rotating collapsar model with two neutrino signals. The first consists predominantly of electron neutrinos with high energies  $\langle E \rangle_{\nu_e} \sim 40$  MeV, while the second is close in its parameters to the standard scenario [10].

The neutrino energy characteristics in the rotational mechanism were considered, for example, in [14, 15]. It was shown that the typical energy could indeed reach 40 MeV under certain conditions. To elucidate the sensitivity of the results obtained to this specific value, we additionally considered the case with an intermediate energy of 30 MeV.

The paper is structured as follows. First we describe LSD and then the neutrino–detector material interaction channels. Next, we provide the characteristics of the unique LSD event at 2:52 UT. Subsequently, we describe the detector response simulation method. The simulation results are presented in the form of energy spectra for the main reactions and in a summary table for the interactions of different types of neutrinos with energies of 15, 30, and 40 MeV. In conclusion, we discuss the results for both SN1987A explosion scenarios under study.

Everywhere below we will call a single energy release in the detector possessing all of the characteristic signatures of a neutrino interaction a “pulse” and a set of such pulses close in time an “event”.

## 2. LSD DESCRIPTION

The liquid scintillation detector (LSD) that operated since 1984 was designed to detect neutrinos from stellar collapses [16]. It was built in collaboration with the Institute for Nuclear Research of the Academy of Sciences of the USSR (presently the Institute for Nuclear Research of the Russian Academy of Sciences) and the Institute of Cosmogeophysics of the Italian National Research Council in the tunnel under Mont Blanc at a depth of 5200 m w.e. Such a soil thickness above the detector provides a reduction in the cosmic-ray muon flux by six orders of magnitude. The 12-km-long road tunnel linking Italy and France passes from the southeast to the northwest.

LSD consisted of 72 scintillation counters  $1.0 \times 1.5 \times 1.0$  m<sup>3</sup> each. The counter box was made of 0.4-cm thick stainless steel. The counters formed three three-level sections (columns) in the form of a parallelepiped with an area of  $6 \times 7$  m<sup>2</sup> and a height of 4.5 m (see Figs. 4–6 below).

Iron containers placed on one another and holding two counters each comprised the detector structure. The walls of the containers had different thicknesses in order that there be a 2-cm layer of iron between the adjacent faces of the counters in the column. The side walls facing the corridors and the bottoms of the containers had a thickness of 2 cm. Thus, given the 0.4-cm thickness of the counter walls, the scintillator of the counters in the column was separated by 2.8-cm layers of iron. The layer of iron was 2.8 cm between the scintillators of the neighboring columns and 4.4 cm between the rock soil and the scintillator. The detector stood on a 10-cm-thick iron platform. To reduce the influence of natural soil radioactivity, the chamber walls were coated with steel plates with a total weight of about 114 t.

There was a space 6 cm in height above and below the detector where it was intended to place two layers of resistive streamer tubes for experiments on muon physics, but with the appearance of the NUSEX project in 1982 [17] capable of solving these problems, it was decided to abandon the resistive streamer tubes.

The scintillator based on white spirit  $C_nH_{2n}$ ,  $\langle n \rangle \approx 9.6$ , contained PPO (1 g/L) and POPOP (0.03 g/L). Each counter was viewed by three FEU-49B photomultiplier tubes (PMTs) with a photocathode diameter of 15 cm. The total signal of three PMTs produced by approximately 15 photoelectrons corresponded to an energy release of 1 MeV in the counter. The energy releases in the counter were analyzed when the signals from three PMTs coincided with a resolution time of 200 ns.

The energy threshold of the 16 internal counters better shielded from the background was  $E_{\text{HET}}^{\text{in}} = 5$  MeV; the detection threshold for the external 56 counters was  $E_{\text{HET}}^{\text{ex}} = 7$  MeV. A pulse from the coincidence circuit of any of the 72 counters was a trigger for the entire detector. In this case, the pulse amplitude (with an energy release above  $E_{\text{LET}} = 0.8$  MeV) and time in a time window of 500  $\mu\text{s}$  were recorded in each of the 72 counters.

The energy calibration of the counters was performed based on the peaks from the energy releases of atmospheric muons (175 MeV for vertical muons) and gamma-ray photons from the captures of neutrons (spontaneous  $^{252}\text{Cf}$  fission products) by hydrogen ( $E_\gamma = 2.2$  MeV) and nickel ( $E_\gamma \approx 9$  MeV) nuclei.

The energy resolution of a scintillation counter is described by the formula

$$\frac{\sigma}{E} = \frac{1}{2.35} \left[ 0.26 \pm \sqrt{\frac{0.31}{E(\text{MeV})} + 0.055} \right], \quad (1)$$

It is based on the determination of the resolution  $\eta = \Delta E/E$ ,  $\Delta E = 2.35\sigma$ ,  $\sigma = 1/\sqrt{N_{\text{pe}}} = 1/\sqrt{aE}$ , where  $\Delta E$  is the full width at half maximum of the resolution function (quasi-Gaussian),  $\sigma$  is the confidence interval (68% measurement error),  $N_{\text{pe}}$  is the number of photoelectrons on three PMTs, and  $a$  is the number of photoelectrons on three PMTs from an energy release of 1 MeV. The first term in parentheses represents the scatter of the light collection coefficient as a function of the burst location in the counter; the first and second terms of the sum under the radical are determined by the fluctuations in the number of photoelectrons  $N_{\text{pe}}$  and the PMT gain unbalance, respectively.

### 3. SELECTION OF CANDIDATES FOR SIGNAL DETECTION

The detection system of the LSD experiment allowed one to detect electron antineutrino ( $\bar{\nu}_e$ )-scintillator interaction products: positrons from the reaction  $\bar{\nu}_e + p \rightarrow n + e^+$  (the Reines-Cowan IBD reaction) and gamma-ray photons from the capture of a neutron by protons  $n + p \rightarrow d + \gamma$  or iron nuclei  $n + \text{Fe} \rightarrow \text{Fe} + \sum \gamma$ . This sequence of reactions gives the main antineutrino detection “signature”.

If a positron is detected, then the amplitude is equal to the sum of the positron kinetic energy and the  $e^+e^-$  annihilation gamma-ray photon energy ( $\sim 1$  MeV).

The particle detection system is determined by the upper,  $E_{\text{HET}}$ , and lower,  $E_{\text{LET}}$ , threshold functions and the edge effect [18].

The mean counting rate of detector trigger pulses is about 45 per hour. The mean number of neutron-like pulses in a time window of 500  $\mu\text{s}$  is 0.1 and 0.8 for the internal and external counters, respectively.

A neutrino burst is identified by the appearance of a series of pulses with an amplitude greater than  $E_{\text{HET}}$  in a time  $t < 20$  s. The detector background can imitate a true event. The background imitation frequency was estimated in an online detector data analysis,

$$F_{\text{im}} = m \frac{(mt)^{k-1}}{(k-1)!} \exp(-mt), \quad (2)$$

where  $m$  is the frequency of background pulses,  $t$  is the pulse packet duration, and  $k$  is the number of pulses. The information about a series of pulses with a low imitation frequency (less than  $1/(5 \div 50)$  years) was sent to printout from the detector computer.

The procedure for the selection of pulse candidates for neutrino signals from gravitational collapses is described in detail in [19, 20].

### 3.1. Neutrino–LSD Material Interaction Reactions

Apart from the IBD reaction, LSD was able to detect particles from the interaction of neutrinos with carbon and iron nuclei in the detector scintillator and structure. The reactions and detection thresholds are given in Tables 1 and 2. The detector can record the delayed pulses (gamma-ray photons and neutrons) from the deexcitation of Mn, Fe and Co nuclei owing to the low threshold  $E_{\text{LET}}$ , which “opens” all counters for reading after the arrival of a trigger, a pulse higher than  $E_{\text{HET}}$ . The pulses from these gamma-ray photons and the gamma-ray photons from the captures of neutrons by the detector iron in the reactions of  $\tilde{\nu}_e(\nu_e)$  with the detector material and surrounding soil can have energies up to 15 MeV and can also be recorded by the detector as single triggers.

**Table 1.** Charged-current (CC) neutrino interaction reactions

Type of neutrinos	Nucleus: C	Nucleus: Fe
$\tilde{\nu}_e$	$\tilde{\nu}_e + {}^{12}\text{C} \rightarrow {}^{12}\text{B} + e^+ (E_{\text{th}} = 14.4 \text{ MeV})$ ${}^{12}\text{B} \rightarrow {}^{12}\text{C} + e^- + \tilde{\nu}_e$	$\tilde{\nu}_e + {}^{56}\text{Fe} \rightarrow {}^{56}\text{Mn}^* + e^+ (E_{\text{th}} = 12.5 \text{ MeV})$ ${}^{56}\text{Mn}^* \rightarrow {}^{56}\text{Mn} + \gamma$ ${}^{56}\text{Mn}^* \rightarrow {}^{55}\text{Mn} + n$ ${}^{56}\text{Mn}^* \rightarrow {}^{55}\text{Cr} + p$
$\nu_e$	$\nu_e + {}^{12}\text{C} \rightarrow {}^{12}\text{N} + e^- (E_{\text{th}} = 17.3 \text{ MeV})$ ${}^{12}\text{N} \rightarrow {}^{12}\text{C} + e^+ + \nu_e$	$\nu_e + {}^{56}\text{Fe} \rightarrow {}^{56}\text{Co}^* + e^- (E_{\text{th}} = 10 \text{ MeV})$ ${}^{56}\text{Co}^* \rightarrow {}^{56}\text{Co} + \gamma$ ${}^{56}\text{Co}^* \rightarrow {}^{55}\text{Co} + n$ ${}^{56}\text{Co}^* \rightarrow {}^{55}\text{Fe} + p$

**Table 2.** Neutral-current (NC) neutrino interaction and electron scattering (ES) reactions

Type of neutrinos	Nucleus:: C	Nucleus:: Fe	$e^-$
$\tilde{\nu}_e$	$\nu_i + {}^{12}\text{C} \rightarrow \nu_i + {}^{12}\text{C}^*$	$\nu_i + {}^{56}\text{Fe} \rightarrow \nu_i + {}^{56}\text{Fe}^*$	$\nu_i + e^- \rightarrow \nu_i + e^-$
$\nu_e$	$(E_{\text{th}} = 15.1 \text{ MeV})$	$(E_{\text{th}} = 15 \text{ MeV})$	
$\tilde{\nu}_{\mu,\tau}$	${}^{12}\text{C}^* \rightarrow {}^{12}\text{C} + \gamma$	${}^{56}\text{Fe}^* \rightarrow {}^{56}\text{Fe} + \gamma$	
$\nu_{\mu,\tau}$	${}^{12}\text{C}^* \rightarrow {}^{11}\text{C} + n$	${}^{56}\text{Fe}^* \rightarrow {}^{55}\text{Fe} + n$	
	${}^{12}\text{C}^* \rightarrow {}^{11}\text{B} + p$	${}^{56}\text{Fe}^* \rightarrow {}^{55}\text{Mn} + p$	

## 4. THE EVENT RECORDED BY LSD DURING THE SN1987A EXPLOSION

A series of five pulses was recorded in the LSD experiment in 7 s on February 23, 1987, at 2 h 52 min Universal Time (UT). Information with signal characteristics was sent to the International Astronomical Union (IAU) on February 28 [2, 21]. Below, the pulses near 2:52 UT will be called the first signal.

The Kamiokande II collaboration (Japan, USA) reported the detection of neutrinos from SN 1987A in the IAU on March 6 and prepared a publication [5]. The team of the IMB experiment (USA) sent the same report to the IAU on March 11 and prepared a publication on March 12 [4]. The group of the Baksan Underground Scintillation Telescope (BUST) [3] reported the extraction of a neutrino signal from their data on April 6. With the corrections for the clock accuracy, all three signals occurred simultaneously at 7:35 UT. LSD recorded two pulses at 7:35 UT [2]. The pulses near 7:35 UT will be called the second signal.

The technique of the experiments of both KII and IMB Cherenkov detectors and BUST scintillation telescope did not allowed one to identify precisely the  $\tilde{\nu}_e p$  interactions: the detectors could not detect an np capture and, thus, in contrast to LSD, had no signature of this reaction.

The KII signal containing 11 pulses (initially 12) was interpreted by the authors as the one produced by  $\tilde{\nu}_e p$  interactions based on approximate isotropy of the direction of particle tracks in the pulses. The authors explained the fact that the particle tracks in 7 of the 11 pulses were directed to the forward hemisphere by fluctuations. The situation with the IMB signal is similar: 7 of the 8 tracks were also directed to the front hemisphere. The KII authors assumed that 2 of the 11 pulses in their signal could be produced by  $\nu e$  scattering, but such a number of  $\nu e$  interactions led to a contradiction with the theoretical predictions about the total energy of the neutrino flux [22–24].

Thus, the recorded LSD cluster contained 5 pulses in the time interval of 7 s bounded by the first and last pulses (Fig. 1). The cluster candidates followed at LSD with a frequency of about 0.5 per day, but this cluster

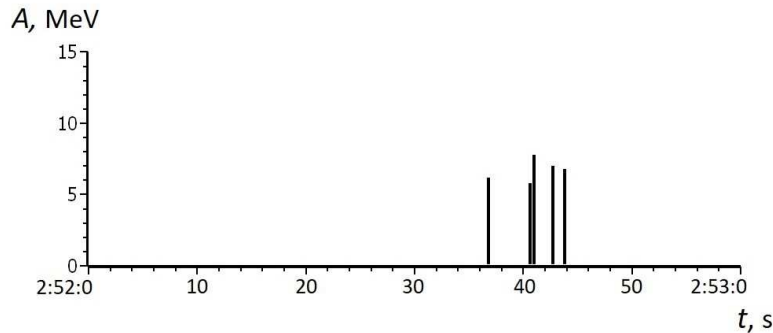


Fig. 1. The series of pulses recorded in the LSD (2 h 52 min UT)

had an exceptionally low background imitation frequency  $F_{\text{im}} \sim 1.8 \times 10^{-3}$  per day and appeared for the first time since the beginning of the detector operation in January 1985. A cluster close in imitation frequency ( $\sim 4 \times 10^{-3}$ ) was recorded only on April 27, 1986; it consisted of 11 pulses in 67 s [25].

The occurrence times of the pulses in LSD and their amplitudes (refined after additional calibrations [20]) are given in Table 3. Only one of the five measured pulses was accompanied by a neutron-like pulse offset from the trigger signal in the detector by  $278 \mu\text{s}$  with an energy of 1.4 MeV.

Table 3. Characteristics of the recorded LSD cluster

Counter number	Pulse time, hour.min.sec	Amplitude, MeV	Neutron-like pulse
31 external	2.52.36.792	6.2	—
14 internal	2.52.40.649	5.8	—
25 external	2.52.41.007	7.8	+1.0 after $278 \mu\text{s}$
35 internal	2.52.42.696	7.0	—
33 internal	2.52.43.800	6.8	—

For information, Table 4 presents the times and the numbers of pulses in the IMB [5], KII [4], and BUST [3] detectors. Such a small number of pulses was caused not only by the distance to the source ( $\sim 50$  kpc from the Earth), but also by the relatively small sizes of the detectors.

## 5. SIMULATION OF THE LSD RESPONSE

The simulation was performed using the GEANT4 software package of version 10.3 [26]. This software package allows detailed simulations of the passage of elementary particles through matter to be carried out by the Monte Carlo method. GEANT4 also has the necessary tools for specifying objects of complex geometry and includes a wide set of theoretical models describing the interaction of elementary particles with matter. A

**Table 4.** The signals recorded by the IMB, KII, and BUST detectors

Detector	First–second pulse times, hour.min.sec	Number of pulses
IMB	7.35.35 – 7.35.47	12
KII	7.35.41 – 7.35.44	8
BUST	7.36.06 – 7.36.21	6

detailed description of the set of physical models applied in our simulations can be found in [27]. It should be noted that these physical settings were specially selected and optimized to simulate the experimental setups in underground low-background laboratories. The testing and debugging were performed on a series of experimental data, from relatively simple experiments on the interaction of protons and  $\pi$ -mesons of fixed energy with iron and lead targets to more complex experimental setups with liquid-scintillator-based detectors at the Artemovsk Scientific Station of the Institute for Nuclear Research in plaster (25 m w.e.) and salt (316 and 570 m w.e.) mines. The results obtained in our numerical simulations agreed well with the results of experiments [28].

There are no models to describe the neutrino–matter interaction in the GEANT4 library package. Therefore, information about the processes involving neutrinos should be added to the simulation from outside. We used standard formulas (see, e.g., [29]) to describe the following processes: (1) neutrino capture by a nucleus, (2) inelastic neutrino scattering by a nucleus, and (3) electron scattering. The main problem here is to calculate the amplitude and distribution of Gamow–Teller and Fermi resonances in the daughter nucleus, which dominate in these processes on nuclei at the typical neutrino energies under consideration. For a full calculation we need information on the neutrino interaction both in the detector scintillator and in the LSD protective metal structures and the soil surrounding the detector. Below we present a compilation of the bibliographic data on the elements (with isotopes) involved:  $^1\text{H}$  [29–31],  $^{12,13}\text{C}$  [32–36],  $^{16,18}\text{O}$  [35, 37–41],  $^{27}\text{Al}$  [42, 43],  $^{28}\text{Si}$  [44, 45],  $^{50,52-54}\text{Cr}$  [46–49],  $^{54,56,57}\text{Fe}$  [33, 34, 40, 50–54],  $^{58,60}\text{Ni}$  [35, 53, 54].

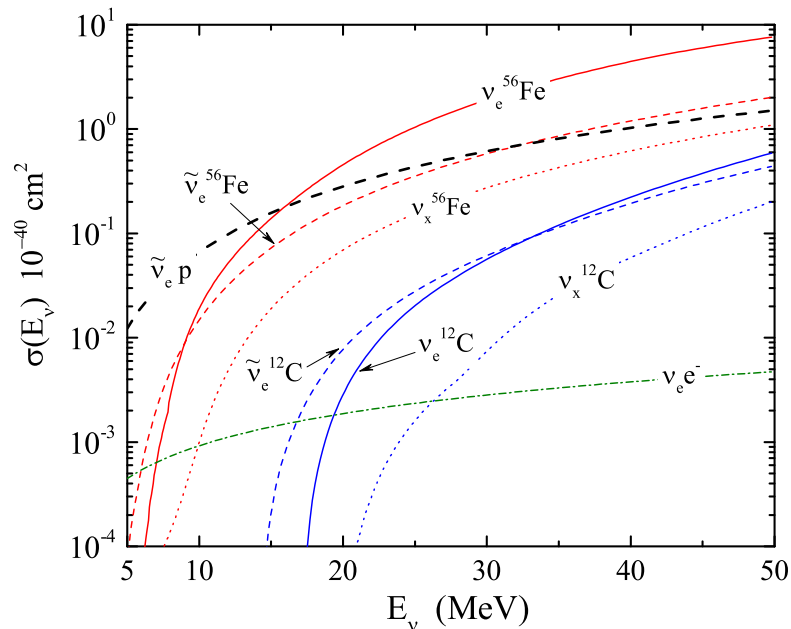
**Fig. 2.** Cross sections for the neutrino interaction with several selected targets as a function of energy

Figure 2 presents the calculated cross sections for the interaction of neutrinos and antineutrinos with several most important targets: hydrogen and carbon nuclei (the scintillator composition is  $C_nH_{2n}$ ), iron (the protective and bearing structures of the detector), and electrons. The solid and dashed lines indicate the results for the interaction of electron neutrinos and antineutrinos via the charged channel, respectively. The dotted and dash-dotted lines indicate inelastic scattering and electron scattering, respectively. As can be seen, the cross section for the reaction  $\nu_e + {}^{56}\text{Fe}$  exceeds the cross section for the main IBD reaction already at about 15 MeV. This is particularly important for the rotational SN explosion mechanism under consideration [12], which can produce high-energy neutrinos.

To demonstrate the uncertainty with regard to the calculated cross sections available in the literature, Table 5 gives the cross sections for the neutrino interaction with an iron nucleus  $\nu_e + {}^{56}\text{Fe} \rightarrow {}^{56}\text{Co} + e^-$  at neutrino energy  $E_\nu = 40$  MeV, according to some works. As can be seen, the available data allow us to find the cross sections to within the accuracy of factor 2. This should be taken into account in the subsequent analysis of our results. Note, however, that the main detection channel, the electron antineutrino–hydrogen interaction reaction, does not contain such uncertainties.

**Table 5.** Cross section for the neutrino interaction with an iron nucleus at  $E_\nu = 40$  MeV

Reference	$\sigma_\nu, 10^{-40} \text{ cm}^2$
[55]	3.72
[40]	5.41
[50]	2.1
[52]	3.04
[56]	4.2
This paper	4.3

### 5.1. LSD Design and the Surrounding Soil

Particular attention and much effort were given to the creation of the LSD geometry. Where possible, it was necessary to include all of the structural elements that could affect the numerical simulation results in the model. The simulated geometry also took into account the granite surrounding the detector. The granite of the Mont Blanc range is composed mainly of silicon dioxide  $\text{SiO}_2$ . The chemical composition of the granite used in our computations and the mass fractions of the main chemical elements are shown in Tables 6 and 7.

**Table 6.** Chemical composition of granite

Compound	Mass fraction, %
$\text{SiO}_2$	72.76
$\text{Al}_2\text{O}_3$	13.96
$\text{K}_2\text{O}$	4.35
$\text{Na}_2\text{O}$	3.76
$\text{Fe}_2\text{O}_3$	2.18
$\text{CaO}$	1.09
$\text{H}_2\text{O}$	0.99
$\text{MgO}$	0.65
$\text{TiO}_2$	0.26

**Table 7.** Mass fractions of chemical elements

Element	Mass fraction, %
O	49.23
Si	34.01
Al	7.39
K	3.61
Na	2.79
Fe	1.53
Ca	0.78
Mg	0.39
Ti	0.16
H	0.11

Since LSD is well shielded from various background sources, the only neutrino–granite nuclei interaction products that could reach the inner detector volume and lead to signal detection by its counters are neutrons.

Therefore, in our preliminary computations we studied the penetrability of neutrons in the granite. As our simulation for various initial neutrino energies (from 1 to 20 MeV) showed (see Fig. 3), the maximum penetration depth does not exceed 1.5 m, and only about 5% of the neutrons traverse a distance more than 100 cm. Therefore, in our computations the granite layer sensitive to the interaction with neutrinos had a thickness of 1 m. In contrast, the total thickness of the granite surrounding the room with LSD and the adjacent segment of the road tunnel in the numerical geometry was 3 m.

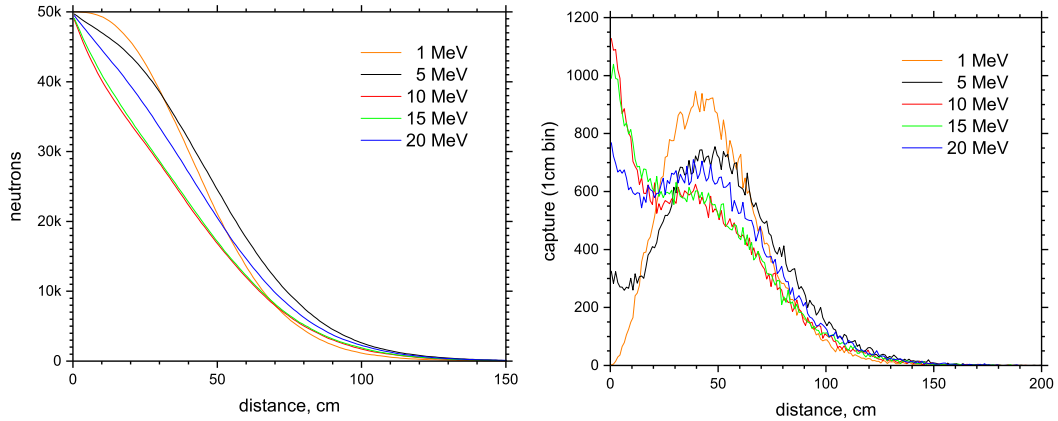


**Fig. 3.** Left: change in the number of neutrons as one recedes from the source point in the granite. Right: the distribution of neutron capture points in the granite as a function of distance.

A general view of the geometry for LSD with an inner detecting volume (counters in iron containers), outer protective steel plates, and a granite layer around the experimental room, and the tunnel fragment is presented in Fig. 4. The internal structure of the detector surrounded by a 1-m granite layer is shown in more detail in Figs. 5 and 6. In our computations the detector geometry is a set of separate volumes with a complex

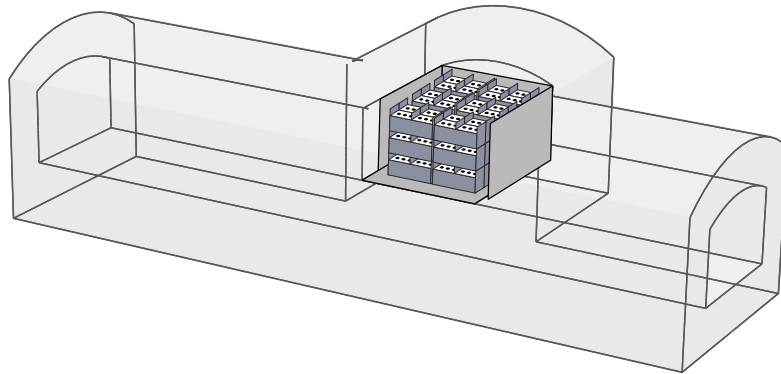


**Fig. 4.** General view of the numerical LSD geometry used in our simulations

shape that are created through logical operations from a set of elementary geometric figures (cylinders, cones, parallelepipeds, etc.). Homogeneous chemical composition and density are specified within a single volume. The precomputed cross sections for the reactions of neutrinos with various nuclei (see above) were used to simulate the interaction of neutrino radiation with the LSD structural elements.

## 5.2. Calculation of the Neutrino Interaction with the Detector Elements

Consider some volume of the experimental setup geometry with index  $i$ , total mass  $M^i$ , and chemical composition specified by the mass fractions  $X_{A,Z}^i$  of the individual nuclei in its chemical composition. Here,  $Z$



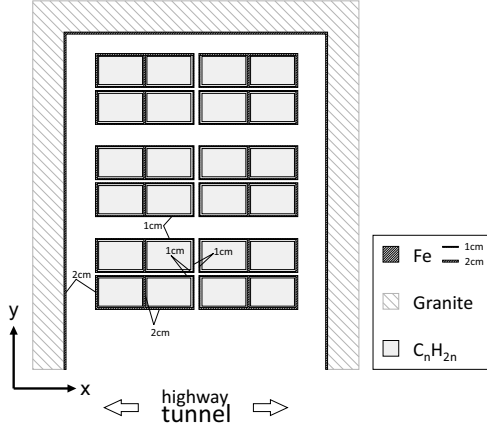


Fig. 5. LSD geometry (top view)

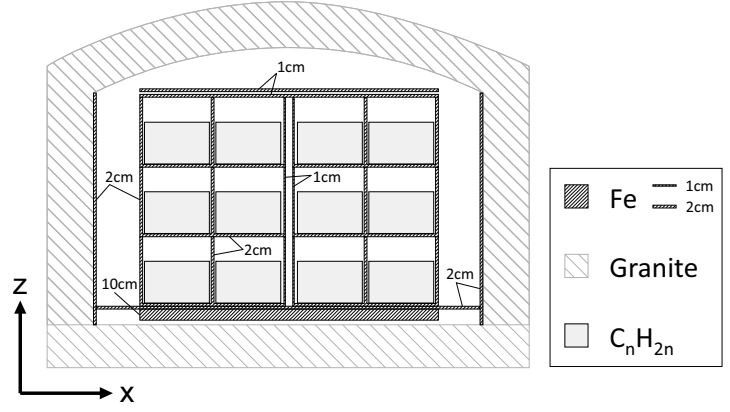


Fig. 6. LSD geometry (a view from the road tunnel)

and  $A$  are the nuclear charge and mass number, respectively. The number of neutrino interactions via a given channel of reactions  $q$  with a nucleus  $(A, Z)$  in the volume  $i$  under consideration per unit flux of neutrinos of a given type is then

$$N_{A,Z}^i = \frac{M^i X_{A,Z}^i}{m_u A} \sigma_{A,Z}^q(E_\nu), \quad (3)$$

where  $\sigma_{A,Z}^q$  is the cross section for the corresponding reaction, and  $m_u$  is the atomic mass unit. As is easy to understand, the total number of reactions (again per unit flux) of neutrinos with energy  $E_\nu$  via channel  $p$  with the matter of a given volume will be

$$N^i = \sum_{A,Z} N_{A,Z}^i = \frac{M^i}{m_u} \sum_{A,Z} \frac{X_{A,Z}^i}{A} \sigma_{A,Z}^q(E_\nu), \quad (4)$$

while the total number of interactions with the detector as a whole is defined by the obvious expression

$$N_{\text{tot}} = \sum_i N^i. \quad (5)$$

The probability that the reaction will occur in volume  $i$  is given by the ratio of Eqs. (4) and (5). A similar simulation of the nucleus with which the neutrino interacts follows next in our computation. The probability of the reaction with a nucleus  $(A, Z)$  is equal to the ratio of (3) to (4). The reaction products (daughter nuclei, possibly, in an excited state, electrons/positrons, etc.) are used as primary particles in our computation using GEANT4. The results obtained are normalized to the total number of neutrino reactions with the simulated detector geometry that is calculated based on a specified neutrino flux. For example, for monochromatic neutrinos with energy  $E_\nu$  from SN1987A, provided that the total energy released isotropically in the form of such neutrinos was  $E_{\text{tot}}$ , the number of interactions can be estimated from the formula

$$N_{\text{int}} \approx 1.2 \frac{E_{\text{tot}}}{10^{53} \text{ erg}} \frac{10 \text{ MeV}}{E_\nu} \frac{M_{\text{tot}}}{100 \text{ t}} \left( \frac{51.4 \text{ kpc}}{R_{\text{SN}}} \right)^2 \sum_{A,Z,q} \frac{X_{A,Z}}{A} \frac{\sigma_{A,Z}^q(E_\nu)}{10^{-42} \text{ cm}^2}, \quad (6)$$

where  $R_{\text{SN}}$  [kpc] is the distance to the SN. Generally, however, it is necessary to integrate over the spectrum of incoming neutrinos.

The data acquisition and signal detection in the counters during our numerical simulation were performed by a technique similar to the operation of the recording equipment in an experiment.

## 6. RESULTS

### 6.1. Simulation of the LSD Response to Neutrino Fluxes from the Soil

At the first stage of our simulation we investigated the assumption about the connection of the signal recorded with LSD at 2:52 UT with neutrons that could be produced in the reactions of the interaction of neutrinos with the granite that surrounded the detector.

First, we studied the penetrability of neutrons in the soil (see Fig. 3 above) to estimate the effective volume (and mass) of the granite that could affect the detector. The penetration depth was  $\sim 100$  cm for the entire range of possible neutron energies. It should be noted that the neutrons still need to traverse more than 4 cm of the iron shield after their escape from the granite. Nevertheless, the granite volume in which the neutrons that are able to escape into the room with the experimental setup can be produced is quite impressive. The granite mass in this volume is more than 3000 t, which exceeds the mass of all iron and steel structures by almost an order of magnitude.

Second, we simulated the detector response to neutrons coming from the granite. These simulations also showed a weak dependence of the results on the initial neutron energy. As an example, we provide the energy distribution of the signals recorded by the LSD counters for two initial energies, 1 and 8 MeV (see Fig. 7). As can be seen, the results agree satisfactorily in energy with the experimental data, which makes the assumption [13] about the possible role of the granite in explaining the recorded signal very plausible. However, despite the large mass of the granite that surrounded the detector, our simulations of the interaction with neutrino radiation showed that neutrons are a very rare product in all of the possible reactions of neutrinos with nuclei in the granite, which does not allow the number of recorded pulses to be explained at all (see Table 8 below).

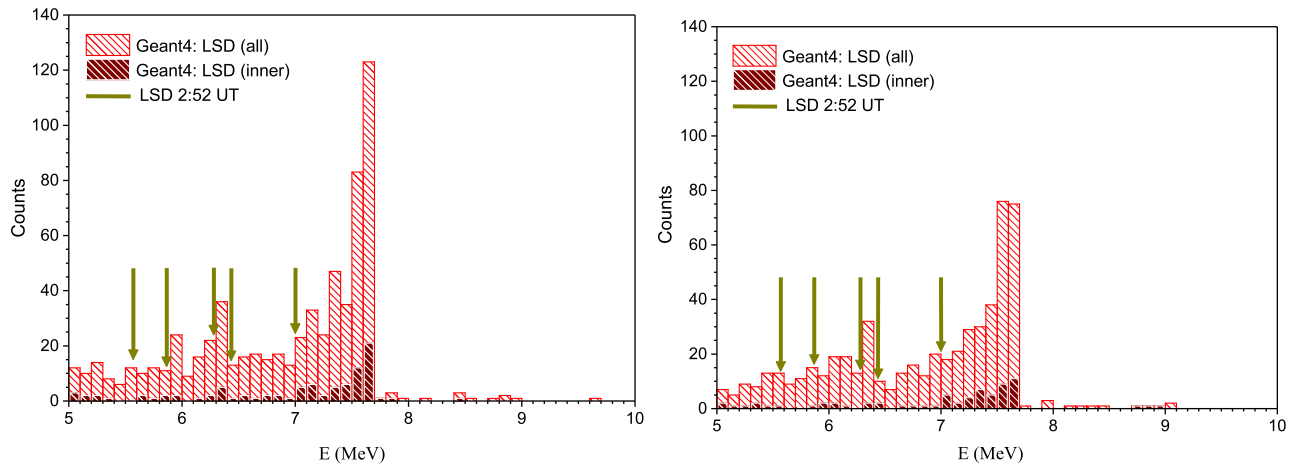


**Fig. 7.** Spectrum of energy releases (with an energy above 5 MeV) in the LSD counters for the neutrons with an initial energy of 1 (left) and 8 (right) MeV produced in the granite. The energy distribution for the internal and all detector counters is indicated by the dark and light colors, respectively. The arrows indicate the energies of the signals recorded in LSD at 2:52 UT

### 6.2. Simulation of the LSD Response to the Neutrino Burst

We performed a series of simulations using the technique described above for various neutrino energies, types, and reaction channels. During the simulation the detector and its surrounding soil were irradiated by a neutrino flux of specific composition (with an energy that was fixed or distributed over the equilibrium spectrum). The total energy radiated by the SN in the form of neutrinos in all our simulations was  $10^{53}$  erg. Figure 8 presents the simulation results for a flux of electron antineutrinos with an energy distributed over the equilibrium spectrum,

$$F_\nu(E_\nu) \propto E_\nu^3 \exp\left(-\frac{3E_\nu}{\langle E_\nu \rangle}\right), \quad (7)$$

with a mean value of  $\langle E_\nu \rangle = 15$  MeV for the charged current reaction channel. The spectrum of energy releases in the counters has a maximum at energies near 7–8 MeV and a slowly decaying “tail”. We simulated 50000 reactions of neutrinos with specified properties. As expected, most of the reactions that led to the detection of signals with an energy above 5 MeV in the scintillation counters occurred in the scintillator itself, while the main nucleus that entered into the reactions with neutrinos was hydrogen (note that the scale in upper panels of Fig. 8 is logarithmic).

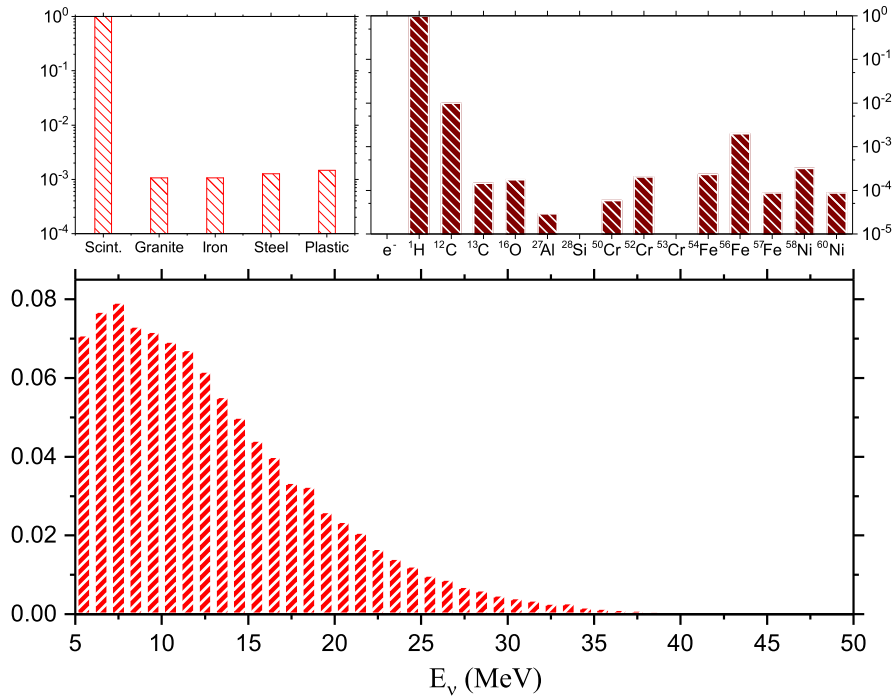


**Fig. 8.** The relative number of reactions in various materials (upper left) and on various nuclei (upper right) accompanied by the detection of a signal with an energy above 5 MeV. Bottom panel: the normalized spectrum of energy releases in the counters for electron antineutrinos with an energy distributed over the equilibrium spectrum with a mean value of 15 MeV in the charged-current reactions

Figure 9 presents the same data, but for a flux of electron neutrinos with an energy distributed over the equilibrium spectrum with a higher mean energy of 40 MeV (see [12]) in the charged-current reactions. The spectrum of energy releases in this case turns out to be fairly extended (approximately to 50 MeV) and monotonically decaying. Neutrinos mostly react with the material of the iron and steel detector structures, but a comparable number of reactions occur in the scintillator as well. Iron and carbon isotopes are the nuclei that enter into the reactions with neutrinos most often.

Finally, Fig. 10 shows the simulation results for the channel of neutral-current and electron scattering reactions. The neutrino spectrum is an equilibrium one with a mean energy of 40 MeV. The spectrum of energy releases has a pronounced maximum in the energy range 5–10 MeV, closely corresponding to the energies recorded in the experiment. Nevertheless, it is still worth noting that there are signals with high energies (up to  $\sim 30$  MeV) in the spectrum as well. As in the previous case, the iron, steel, and scintillator play a major role. However, apart from the iron and carbon isotopes, the reactions of neutrino scattering by electrons contribute noticeably to the number of recorded pulses.

Table 8 summarizes the most important results of our numerical simulations for a wide set of neutrino energies and types of reactions. The distance to the neutrino radiation source was set equal to the distance to SN1987A. At the same time, the neutrino flux was assumed to be isotropic, while its total energy in each simulation was  $10^{53}$  erg. Table 8 gives the expected (from the simulation results) number of pulses in LSD, the probability that a given energy release fell into the range 5–10 MeV, the fraction of pulses from the reactions in the granite, and the fraction of pulses from the reactions among the products of which there were neutrons.

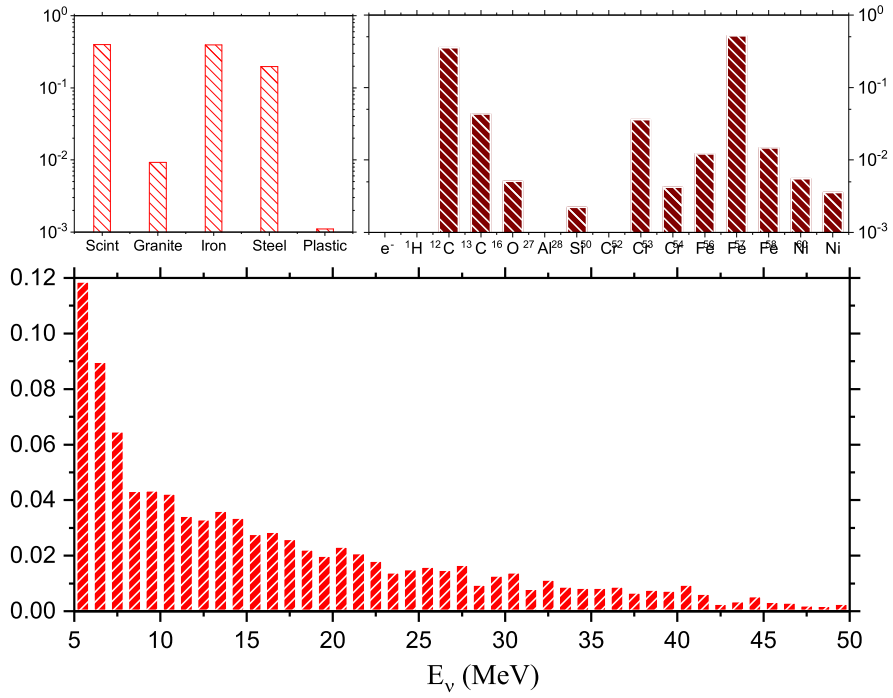


Fig. 9. Same as Fig. 8, but for electron neutrinos with an energy distributed over the equilibrium spectrum with a mean value of 40 MeV in the charged-current reactions.

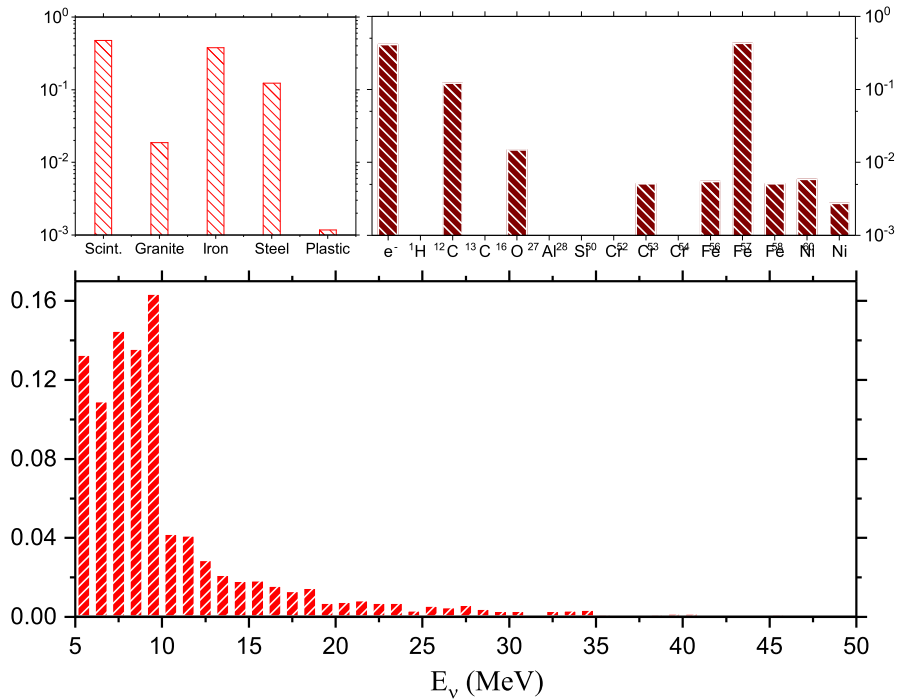


Fig. 10. Same as Fig. 8, but for electron neutrinos with an energy distributed over the equilibrium spectrum with a mean value of 40 MeV in the charged-current reactions

As can be seen from the last two columns of the table, the contribution of the granite and neutrons to the number of recorded pulses from the neutrino radiation is negligible for all of the possible energies and reaction channels. This is apparently because the granite surrounding LSD is composed mostly of  $\alpha$ -particle nuclei

**Table 8.** Summary table of the simulation results for various types of reactions and energies of neutrinos from SN 1987A

Type of reaction	Mean neutrino energy, MeV	Total number of expected pulses	Probability that one pulse fell into range 5–10 MeV	Fraction of reactions in soil, $\times 10^{-2}$	Fraction of pulses with neutron production, $\times 10^{-2}$
$\tilde{\nu}_e$	15	1.92	0.379	0.11	0.06
	30	5.6	0.175	0.29	0.92
	40	8.46	0.135	0.54	1.96
$\nu_e$	15	0.08	0.635	0.17	1.10
	30	1.1	0.449	0.45	2.43
	40	2.6	0.371	0.93	2.86
$NC+ES$	15	0.046	0.69	0.06	0.68
	30	0.22	0.69	0.92	1.64
	40	0.41	0.69	1.93	3.52

( $^{16}\text{O}$ ,  $^{28}\text{Si}$ , see Table 7) with high binding energies and neutron separation energies. Out of the still produced neutrons, only a small fraction will be able to escape from the soil (see Fig. 3) and an even smaller fraction will be able to traverse the LSD protective structures to give a signal in the counters. Thus, unfortunately, the elegant idea [13] about the influence of the surrounding soil on the signal from the SN detected in LSD does not work.

As can be seen from Table 8, the main factor that increases the total number of recorded events is a high energy. The neutrino scattering reactions contribute insignificantly to the total number of events at all of the possible energies. On the other hand, the spectrum of energy releases observed in the experiment is most closely reproduced precisely in the scattering reactions.

### 6.3. Errors in the Results Obtained

The quantities in Table 8 are affected by the errors in determining some characteristics of the detector and the neutrino flux. The scatter of parameters of different GEANT4 versions also contributes to the systematic error of our simulations.

To reduce the systematic error of our simulations, we performed a sufficiently large number of simulations. For each set of parameters the number of reactions with neutrinos was  $5 \times 10^4$ . This made it possible to bring the statistical error for the main quantities obtained in our simulations (the total number of expected events and the probability of falling into the energy range 5–10 MeV) to fractions of percent. The values of the quantities in the last two columns of Table 8 (the fractions of reactions in the soil and of events with neutron production) were obtained with a lower accuracy, because these events are fairly rare. However, the statistical error did not exceed 20% even for them.

The example with  $^{56}\text{Fe}$  (Table 5) gives an idea of the systematic errors when including a set of neutrino interaction cross sections in the simulations. As can be seen, the difference in cross sections is of the order of a factor of 2 and this quantity depends strongly on the energy and type of nucleus. However, the cross section for the main  $\tilde{\nu}_e p$  reaction is well known.

The error associated with the masses of the materials used in our simulations and the geometry of the detector and the experimental room contribute no more than 12% to the systematic error of the results obtained.

As experience shows, the result also depends to some extent on the GEANT4 version used [28]. This is related to the details of the physics and the parameters of the processes included by the developers in the software package version. In our simulations we used the GEANT4 version 10.3.0.

The main uncertainty is associated with the neutrino burst characteristics used: the total burst energy ( $\sim 10^{53}$  erg), the assumption that the neutrino radiation is spherically symmetric, the energy characteristics of the neutrino fluxes, etc. In the real case of SN1987A, they can differ from those used in the simulations. However, this uncertainty can be partly corrected, depending on the implied SN model: for example, using a different total energy leads simply to a renormalization of the derived numbers of pulses in the detector etc.

## 7. DISCUSSION

Let us discuss the results obtained and compare them with the experimental data. For these purposes, we will use Fig. 11. It presents a compilation of experimental data from four detectors [57]: KII (squares), IMB (circles), BUST (triangles), and LSD (diamonds).

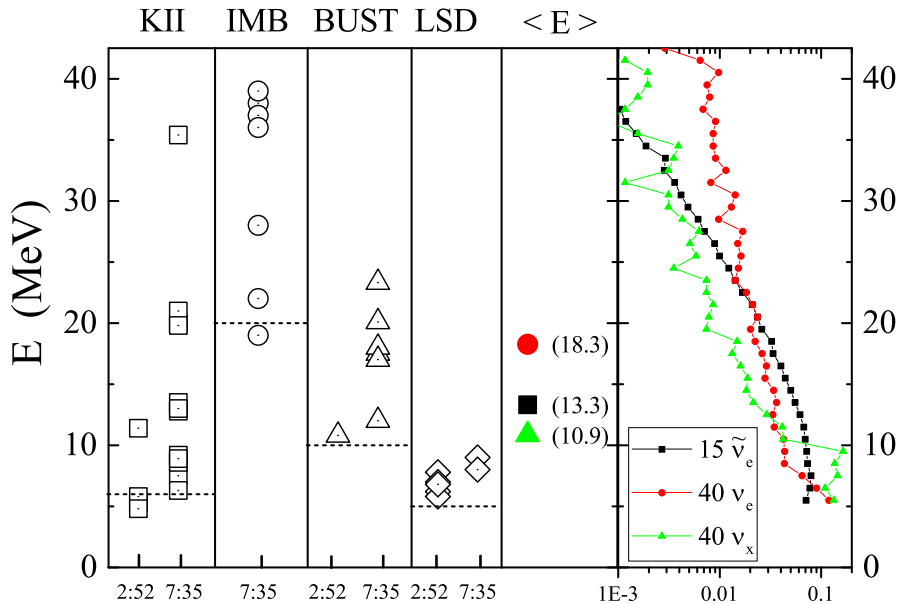


**Fig. 11.** Compilation of experimental data from four detectors: KII (squares), IMB (circles), BUST (triangles), and LSD (diamonds). Only the recorded energies are shown. For all of the detectors, except IMB, the first and second data sets correspond to 2:52 and 7:35 UT, respectively.

(circles), BUST (triangles), and LSD (diamonds). Only the recorded energies are shown. For all detectors, except IMB, the first and second data sets correspond to (approximately) 2:52 and 7:35 UT, respectively. IMB did not “see” the first signal, in contrast to the remaining detectors (for a discussion of the situation with the non-recognition of the reality of the first signal, see [8]). The spectra of energy releases in LSD according to our simulations (Figs. 8–10) and the corresponding mean energies  $\langle E \rangle$  (the numerical value in MeV is given in parentheses) are also shown. The horizontal dashed lines indicate the threshold level for each detector. Here, it is pertinent to recall that the notion of a detection threshold is conventional.

During the second signal at 7:35 UT the number of events in the LSD was 2, in excellent agreement with the value calculated by us for standard collapse (15-MeV antineutrinos) — 1.92 (Table 8).

During the first signal no detector, except LSD, was able to record the signal from electron neutrinos [12]. The fact that KII and BUST still “saw” something (Fig. 11) suggests that there was a slight admixture of low-energy electron antineutrinos in the first signal (there was no pulse at IMB due to a high,  $\sim 20$  MeV, threshold). This means that we can also attribute one of the five pulses in LSD to the detection of the IBD reaction, the one that (alone) was accompanied by a characteristic signature of this event, see Table 3. We assign an energy of 15 MeV to the neutrino that generated this pulse based on the spectrum of energy releases in KII and BUST and the absence of a signal in IMB (Fig. 11).

Let us now consider the main ingredient of the rotational model—high-energy (40 MeV) electron neutrinos. We see that the combination of the numbers of charged-current (2.6) and neutral-current (0.41) pulses gives 3

events, which, given all of the available uncertainties, coincides remarkably with  $5 - 1 = 4$  pulses from electron neutrinos. The 40-MeV muon and tau neutrinos at the time of the first signal in the rotating collapsar model can originate from electron neutrinos due to oscillations.

Thus, the combination of events at the time of the first signal in LSD can appear as:

$$5 = 1(15 \text{ MeV } \tilde{\nu}_e) + 1(40 \text{ MeV } \nu_x) + 3(40 \text{ MeV } \nu_e). \quad (8)$$

Naturally, this is only one of the possible variants, through apparently the most probable one: we cannot increase the fraction and energy in  $\tilde{\nu}_e$ , otherwise other detectors should have recorded much more pulses. In contrast, the neutral-current reactions give a too small number of events due to their small cross section.

However, we see a major problem in the measured energies of the events: all of the energy releases in LSD (in both first and second signals) lie in a narrow range, from 5 MeV (threshold) to approximately 9 MeV. Let us calculate the probability that all five pulses of the combination (8) considered above fell into this range using Table 8:

$$P(5) = 0.379 \times 0.69 \times (0.371)^3 \approx 0.013. \quad (9)$$

Turning to Fig. 11, we see that the signal in LSD indeed breaks out of the general series. In all of the remaining detectors the pulse energy distribution is wide, as it must be (see the mean expected pulse energies in LSD in the same figure). We see that the signal in LSD agrees neither with the computed spectra of energy releases (Figs. 8–10) nor with the pulse energies in other detectors. All five pulses of the first signal in LSD have low energies (see also Table 3), but high energy neutrino ( $\nu_e$  and/or  $\nu_{\mu,\tau}$ ) fluxes are required to explain their number (recall that the neutrino–matter interaction cross section increases with energy approximately as  $\sigma_\nu \sim E_\nu^2$ ).

We can admit an error in the energy calibration of the LSD counters, as a result of which the pulse amplitude will be at least halved. This could explain the energy spectrum of the pulses in LSD, which clearly breaks out of both the spectra of other detectors and the predictions of our simulations. However, this explanation comes into conflict with the agreement between the experimental and computed spectra of muon energy losses (from 40 to 400 MeV) in the counter and with the correspondence of the calibration based on the 2.2-MeV ( $\gamma$ -ray photons from  $np$ -captures) and 9-MeV ( $\gamma$ -ray photons from  $n$ Ni captures) peaks. Unfortunately, the LSD calibration can no longer be checked in the range 10–40 MeV of interest to us (for example, this could have been done with the LINAC calibration system used in Super-Kamiokande [58]), because LSD was dismantled in 1998.

The closeness of the LSD pulse amplitudes to the detection threshold  $\sim 7$  MeV may suggest a “background” origin of the signal. The connection of the change in the background of the experiment (the number of radionuclide decays in the soil surrounding the detector and its materials) with the SN 1987A explosion is discussed in [59].

Nevertheless, the facts that confirm a high significance of the LSD signal remain:

- among the LSD signal candidates for the detection of a  $\nu$ -burst selected over 14 years of operation, this signal has the lowest background imitation probability [60];
- the probability of a chance coincidence of the LSD signal with the SN1987A explosion is extremely low, less than  $< 1.4 \times 10^{-6}$  [61, 62];
- the LSD signal enters into the central part of the unique and unexplainable 6-hour event in the interval approximately from 1 to 7 hours UT on February 23, 1987, formed by the set of experimental data from four neutrino detectors and two gravitational wave detectors in Rome and Maryland that operated during the SN1987A explosion [59, 61].

## 8. CONCLUSIONS

In several aspects the derived quantities are approximate. Nevertheless, based on a detailed simulation of the interactions of neutrinos from the gravitational stellar core collapse with the LSD material and surrounding soil, we can draw the following conclusions.

First, our simulation showed that the number of recorded LSD pulses both at the time of the first burst 2:52 UT and at the time of the second one 7:35 UT could indeed be obtained within the rotational SN explosion mechanism. However, the energy characteristics of both groups of pulses do not correspond to the computed expected spectra of energy releases and the data from other detectors.

Second, the hypothesis suggested in [13] that the signal in LSD at 2:52 UT could be generated by the neutrinos produced by neutrino fluxes in the soil surrounding the detector does not pass a quantitative check. As our simulations showed, the spectra of such pulses are indeed very similar to the LSD data. However, their number is negligible for all of the neutrino radiation parameters considered.

Above we presented several possible explanations for this. At present, there is no explanation that would satisfy all of the data, both theoretical and experimental ones. Nevertheless, we hope that the results presented here will serve as an important step in long-term attempts to elucidate the nature of the unique signal in LSD coincident in time with the SN1987A explosion.

## 9. ACKNOWLEDGMENTS

This study was performed in 2019 and was essentially finished in early 2020, before the death of our coauthors A.S. Malgin and O.G. Ryazhskaya. We think their contribution to this study to be decisive and devote the paper to their memory with gratitude. We thank V.S. Imshennik and D.K. Nadyozhin, who has also passed away, for the useful discussions and sincere interest in this study. We are grateful to the referee whose remarks contributed significantly to an improvement of the text of our paper.

## 10. FUNDING

The work of A.V. Yudin was supported by the Russian Science Foundation (project no. 21-12-00061).

## REFERENCES

1. IAUC 4316: 1987A, N. Cen. 1986. February 24, 1987
2. M. Aglietta et al., EuroPhys. Lett. 3 (1987) 1315
3. E.N. Alekseev et al., Sov. Phys. JETP Lett. 45 (1987) 461
4. R.M. Bionta, et al., Phys. Rev. Lett. 58, 1494 (1987)
5. K. Hirata, et al., Phys. Rev. Lett. 58, 1490 (1987)
6. Ya. B. Zel'dovich and O. Kh. Guseinov, Sov. Phys. Dokl. 10, 524 (1965)
7. W.D. Arnett, Can. J. Phys. 44, 2553 (1966)
8. A. De Rujula, Phys. Lett. B, Vol. 193, N 4, 514 (1987)
9. V.S. Berezinsky, C. Castagnoli, V.I. Dokuchaev, P. Galeotti. Il Nuovo Cimento, 11C, N3, 287 (1988)
10. V.S. Imshennik, Space Sci. Rev. 74, 325(1995).
11. A. Drago, G. Pagliara, Europ. Phys. J. A, 52, 41, 15 pp (2016)
12. V. S. Imshennik and O. G. Ryazhskaya, Astron. Lett. 30, 14 (2004)
13. S. Yen, TRIUMF Vancouver, Canada (talk 18-Apr 2017)
14. V.S. Imshennik V.O. Molokanov, Astron. Lett., **35**, 12, 799–815 (2009)
15. V.S. Imshennik, V.O. Molokanov, Astron. Lett., **36**, 10, 721–737 (2010)



16. Badino G. et al. *Nuovo Cimento* (1984) 7C, 573
17. G. Battistoni et al., *Phys. Lett. B*, **133**, 6, p. 454-460
18. A. Porta “*Energy measurement in LVD to reconstruct Supernova neutrino emission*”. PhD Thesis of Torino University (2005). P.159
19. V. L. Dadykin, G. T. Zatsepin, V. B. Korchagin, et al., *JETP Lett.* 45, 593 (1987).
20. Aglietta, M. et al., “*Search for neutrinos from collapsing stars at Mont Blanc*” In “*Vulcano 1988, Proceedings, Frontier objects in astrophysics and particle physics*” (1989) Vol.19 pp.103-120
21. IAUC 4323: 1987A February 24, 1987
22. LoSecco J.M., *Proceedings of the Second International Symposium UP-87, Baksan, USSR 1987* (Nauka, Moscow) 1988, p. 100.
23. LoSecco J.M., *Phys. Rev. D*, 39, 1013 (1989)
24. A. Malgin, *il Nuovo Cim. C*, 21, 317-329 (1998)
25. N. Yu. Agafonova, A. S. Malgin, and V. Fulgione, *J. Exp. Theor. Phys.* 117, 258 (2013)
26. V.N. Ivanchenko (for Geant4 Collab.), *Nucl. Instrum. Methods A* 502, 666 (2003)
27. K. V. Manukovskii, O. G. Ryazhskaya, N. M. Sobolevsky, and A. V. Yudin, *Phys. At. Nucl.* 79, 631 (2016).
28. K.V. Manukovskiy et al., *Proceedings of the 16th Lomonosov Conference*, p. 72, 2015
29. Burrows A., Thompson T.A. “*Neutrino-Matter Interaction Rates in Supernovae*”. In: Fryer C.L. (eds) *Stellar Collapse. Astrophysics and Space Science Library*, vol 302. Springer, Dordrecht(2004)
30. P. Vogel, *Phys. Rev. D* 29, 9 (1984)
31. A. Strumia, F. Vissani, *Phys. Lett. B*, 564, 1-2, p. 42-54, (2003)
32. T. Yoshida, T. Suzuki, S. Chiba et. al., *Astroph. Journal*, 686, 448–466 (2008)
33. H. Dapo, N. Paar, *Phys. Rev. C* 86, 035804 (2012)
34. E. Kolbe, K. Langanke, P. Vogel, *Nucl. Phys. A* 652 91-100 (1999)
35. T. Suzuki, *Journal of Physics: Conference Series* 321, 012041 (2011)
36. M. Fukugita, Y. Kohayama, K. Kubodera, *Phys. Lett. B*, 212, 2 (1988)
37. E. Kolbe, K. Langanke, P. Vogel, *Phys. Rev. D* 66, 013007 (2002)
38. T. Kuramoto, M. Fukugita, Y. Kohyama and K. Kubodera, *Nucl. Phys. A*, 512, 711-736, (1990)
39. W.C. Haxton, *Phys. Rev. D*, 36, 8, (1987)
40. R. Lazauskas and C. Volpe, *Nucl. Phys. A* 792, 219 (2007)
41. B.D. Anderson, A. Fazely, R.J. McCarthy et al., *Phys. Rev. C* 27, 4 (1983)
42. I. Stetcu, C.W. Johnson, *Phys. Rev. C* 69, 024311 (2004)
43. Y. Fujita, H. Akimune, I. Daito et al., *Phys. Rev. C* 59, 1 (1999)
44. C. Luttge, P. Neumann-Cosel et al., *Phys. Rev. C*, 53, 1, pp.127-130 (1996)
45. B.D. Anderson, N. Tamimi et al., *Phys. Rev. C*, 43, 1 (1991)
46. I. Petermann, G. Martinez-Pinedo, K. Langanke, E. Caurier, *Eur. Phys. J. A* 34, 319 (2007)
47. K. Langanke, G. Martinez-Pinedo, P. von Neumann-Cosel, and A. Richter, *Phys. Rev. Lett.* 93, 202501 (2004)

48. K. Muto, H. Horie, Nucl. Phys. A, 440, 2, p. 254-273 (1985)
49. J. Nabi, R. Shehzadi, M. Fayaz, Astroph. and Space Science, 361, 95, 17 (2016)
50. N. Paar, D. Vretenar and P. Ring, J. Phys. G: Nucl. Part. Phys. 35, 014058 (2008)
51. J. Toivanen, E. Kolbe, K. Langanke, G. Martinez-Pinedo, P. Vogel, Nucl. Phys. A 694, 395–408 (2001)
52. A. Bandyopadhyay, P. Bhattacharjee, S. Chakraborty, K. Kar, S. Saha, Phys. Rev. D 95, 065022 (2017)
53. E. Caurier, K. Langanke, G. Martinez-Pinedo, F. Nowacki, Nucl. Phys. A 653 439-452 (1999)
54. A. Juodagalvis, K. Langanke, G. Martinez-Pinedo et al., Nucl. Phys. A, 747, 87-108 (2005)
55. E. Kolbe and K. Langanke, Phys. Rev. C, 63, 025802 (2001)
56. O.G. Ryazhskaya and S.V. Semenov, Phys. Atom. Nucl., 81, 2, 262–265 (2018)
57. V. L. Dadykin, G. T. Zatsepin, and O. G. Ryazhskaya, Sov. Phys. Usp. 32, 385 (1989)
58. J. Migenda “Supernova Model Discrimination with Hyper-Kamiokande”, PhD thesis, University of Sheffield, arXiv:2002.01649
59. N. Agafonova, A. Malgin, E. Fischbach, arXiv:2107.00265 [nucl-ex]
60. O. G. Ryazhskaya, Phys. Usp. 49, 1017 (2006)
61. P. Galeotti, G. Pizzella, Eur. Phys. J. C 76, 426 (2016)
62. M. Aglietta et al., il Nuovo Cim., C 14, 171-193 (1991)